

THE KINEMATICS AND PHYSICAL CONDITIONS OF WARM IONIZED GAS IN SPIRAL DISKS

Matthew A. Bershadsky¹, David R. Andersen²

¹*University of Wisconsin*, ²*Herzberg Institute of Astrophysics*

Abstract

We present integral-field echelle observations of the warm, ionized phase of the interstellar medium (ISM) of many nearly face-on spiral galaxies. Luminosities and line-widths of H α , [SII] and [NII] reveal several distinct trends in the conditions of the ionized gas. In principle these measures yield estimates for temperature, density, and energy sources of the kinematic heating. The emergent picture is complex: We find variations of the line-widths between galaxies and with galactic radius, and correlations between line-widths and emission-line luminosity and line-ratio. Two related bimodalities appear in line-ratio distributions and in the radial distribution of H α luminosity. We briefly contrast ISM observations of nearby galaxies to the Milky Way and high- z galaxies.

1. Introduction

What drives gas velocity dispersions in star-forming galaxies is still an open question. In dynamically-cold disks it is unclear whether gas moves primarily in response to the local gravitational potential of the disk, cloud-cloud interactions, or is largely driven by a combination of photon-heating and (gravitational and wind-driven) shocks. The situation is complicated by a wide range of physical conditions and surface-brightness, and the need to disentangle geometric effects. The vertical dispersion-component of the ionized gas, which we focus on here, is observationally well-defined (projection issues are minimized in face-on systems), and easily obtained with optical spectroscopy. Understanding the variations of vertical line-widths in dynamically quiescent disks may tell us, in a broader context, what drives line-widths in more extreme systems. One underlying goal is to understand how well random motions of the ionized gas can be used as a dynamical tracer, as has often been used in studies of nearby and distant, star-forming galaxies.

The earliest line-width measurements of the vertical dispersion component in disks were made of HI (van der Kruit & Shostak, 1982, 1984). Their

small amplitudes ($\sigma_{HI} \sim 6\text{-}12$ km/s) and near-constancy with galactocentric radius led to the suggestion that these motions were driven by photon heating. However, Combes & Bequaert (1997) observed similar values of $\sigma_{CO} \sim 6\text{-}9$ km/s for cold, molecular gas, while $H\alpha$ Fabry-Perot studies of ionized gas in $H\text{ II}$ regions yield median values of $\sigma_{H\alpha} \sim 14\text{-}25$ km/s – again, nearly constant with radius (e.g., Rozas et al. 2000). Corrected for thermal broadening, Jimenez-Vicente et al. (1999) found $\sigma_{H\alpha}$ as low as ~ 11 km/s. This suite of observations seems to rule out a purely thermal origin for the vertical heating, but the nature of the “heating” mechanisms and their dependence on gas-phase remains quite unclear. Hints include the density-dependence of the observed $H\text{ I}$ line-widths from the work of van der Kruit & Shostak, and the well-known luminosity-dependence of the observed $H\text{ II}$ line-widths.

Past studies encompass only a handful of nearly face-on galaxies. Optical studies have sampled small filling-factors with long-slit spectrographs, or were limited to emission surface-brightness typically above that of the diffuse component of the warm ionized medium. Here, we take a first step toward understanding the range of ionized-gas vertical velocity dispersions using full, two-dimensional maps of a large sample of normal, nearly face-on disks.

2. DensePak Survey

A sample of 39 nearly face-on spiral galaxies spanning a range of type and luminosity were selected for $H\alpha$ -region echelle observations with the DensePak integral field unit (IFU) on the WIYN telescope. This survey (Andersen et al. 2001, 2003, 2005 and these proceedings) is a precursor to the Diskmass Survey (Verheijen et al., these proceedings), and has the desirable attribute of high spectral resolution ($\lambda/\Delta\lambda = 14,500$) with 3 arcsec spatial sampling.

Gaussian line-fits were made to $H\alpha$ and $[\text{NII}]\lambda\lambda 6548, 6583$ in ~ 5500 fiber spectra. $[\text{SII}]\lambda\lambda 6716, 6730$ were also measured in most galaxies. Few spectra appear to have multi-component, or significantly non-Gaussian lines. Fibers sample $1.1_{-0.2}^{+0.4}$ kpc (median and quartile) diameter footprints for this sample ($H_0 = 70$ km/s/Mpc used throughout). Line-fluxes were well-calibrated by matching the spectral continuum level to calibrated R -band surface-photometry. Effects of beam smearing (< 5 km/s) and instrumental broadening (~ 9 km/s) are small ($< 18\%$; 12% typical), and well calibrated. The following analysis is based on measured line-widths corrected for these effects.

3. Results and Discussion

We find a median vertical dispersion of $\sigma_{H\alpha} \sim 18$ km/s, with a sample distribution that appears constant with radius. However, individual galaxies have different median $\sigma_{H\alpha}$, and some show strong radial trends. These differences correlate with line-strength and line-ratio: Galaxies with low $\sigma_{H\alpha}$ tend

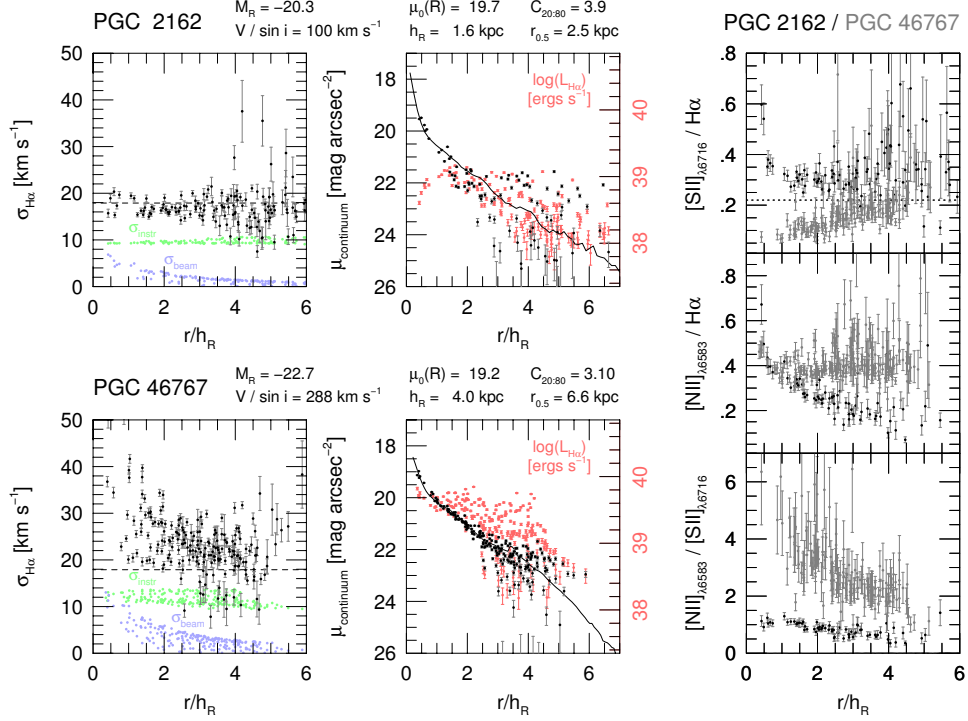


Figure 1. **Left Panels:** $H\alpha$ velocity dispersion vs radius for each fiber observed in two galaxies (marked). Radii are normalized by the disk radial scale length, h_R . Sample median dispersion of 18 km/s is marked by the horizontal, dashed line. Beam-smearing and instrumental resolution for each fiber, also plotted, lie well below most corrected data points. Note differences in mean and radial trends of σ between these two galaxies. These galaxies are otherwise typical of the survey which contains systems with $i < 30$ and sizes ($45'' < D_{25} < 75''$) well-matched to the IFU foot-print, such that maps (typically covering $0.4\text{-}1 \text{ arcmin}^2$) sample out to several disk scale-lengths. **Central Panels:** Continuum fiber flux (dark points; left scale) and $H\alpha$ fiber luminosity (light points; right scale) are over-plotted for the same two galaxies. Solid curves represent the calibrated R-band surface-brightness profiles used to calibrated the spectral continuum flux. Note the increase in $H\alpha$ luminosity in the inner two scale-lengths of PGC 46767, while PGC 2162 plateaus at, or below, $10^{39.2}$ ergs/s, and in fact drops in the very center. In general, this behavior is correlated with the amplitude and radial trend of $\sigma_{H\alpha}$, with $10^{39.2}$ ergs/s in a ~ 1.1 kpc diameter beam being a dividing threshold, as shown in Fig. 2 and 3. **Right Panels:** Line-ratios vs radius for both galaxies are over-plotted to show dramatic differences in mean values and radial trends for these two galaxies. These line-ratio differences correlate with differences in σ and $L_{H\alpha}$ in our sample. These two galaxies are roughly representative of the extremes in the range of galaxies observed. The dashed, horizontal line in the top-right panel at $[SII]/H\alpha = 0.22$ is roughly where Reynolds (1988) notes there is a distinction between H II-like regions and the diffused, ionized gas (DIG) of the Milky Way. There is a bimodality in the distribution of $[SII]/H\alpha$ for the entire sample, with a correlation to the luminosity and rotation speed of the system. This is akin to the results noted by Rubin, Ford, & Whitmore (1984). However, there are galaxies in our sample (e.g., PGC 32638), which straddle this division, and transition from H II-like to DIG-like as a function of radius.

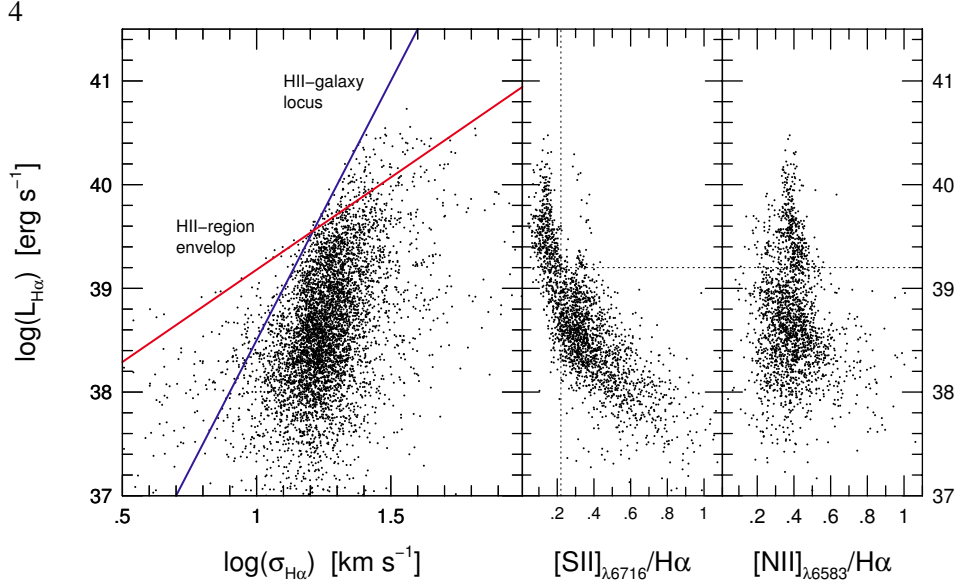


Figure 2. **Left Panel:** $H\alpha$ luminosity vs velocity dispersion for each fiber for all galaxies in our survey. Lines for H II regions and H II galaxies (described in text) bound different portions of the distribution observed in ~ 1.1 kpc diameter apertures. **Right Panels:** $H\alpha$ luminosity vs line-ratios of [SII] and [NII] to $H\alpha$. The strong trend of [SII]/ $H\alpha$ with $L_{H\alpha}$ is seen in MW ISM studies (e.g., Haffner et al. 1999), but the lack of correlation of [NII]/H with $L_{H\alpha}$ is not. Both distributions appear bimodal about $\log(L_{H\alpha})=39.2$ ergs/s (dotted horizontal line).

to have constant dispersion with radius, weak $H\alpha$ emission, and high [SII]/ $H\alpha$ flux ratios. Galaxies with strong radial gradients in $\sigma_{H\alpha}$ have larger $\sigma_{H\alpha}$ values and stronger emission, significantly lower [SII]/ $H\alpha$, and somewhat higher [NII]/ $H\alpha$. Two extreme examples are shown Fig. 1. Sample correlations of line-widths and line-ratios with $L_{H\alpha}$ are shown in Fig. 2.

One puzzle to resolve is why $H\alpha$ Fabry-Perot studies find a much shallower envelop in the σ - $L_{H\alpha}$ distribution for H II regions of individual galaxies (a slope of 1.5-3 in dex; e.g., Relano et al. 2005) than the σ - $L_{H\alpha}$ correlation found for low- and high-redshift H II-galaxies as an ensemble (a slope of ~ 5 in dex, e.g., Melnick et al. 1987; Siegel et al. 2005). Our L - σ distribution (Fig. 2) for all points within all galaxies is well bounded by the H II-region envelop at low sigma (< 16 km/s) and by the H II-galaxy locus at high sigma (> 16 km/s). However, the majority of points fall on a locus which is closer to the H II-galaxy relation although perhaps somewhat steeper. Aperture and selection effects must be considered - something we can model for our survey.

The above correlations produce a strong trend in [SII]/ $H\alpha$ along the L - σ locus: Regions of higher σ and $L_{H\alpha}$ have lower [SII]/ $H\alpha$. This line-ratio trend with luminosity agrees qualitatively with studies of the DIG in the MW (Haffner et al. 1999). Unlike the MW ISM, however, [NII]/ $H\alpha$ does *not* appear to be correlated with $L_{H\alpha}$ overall (although this correlation is seen in some

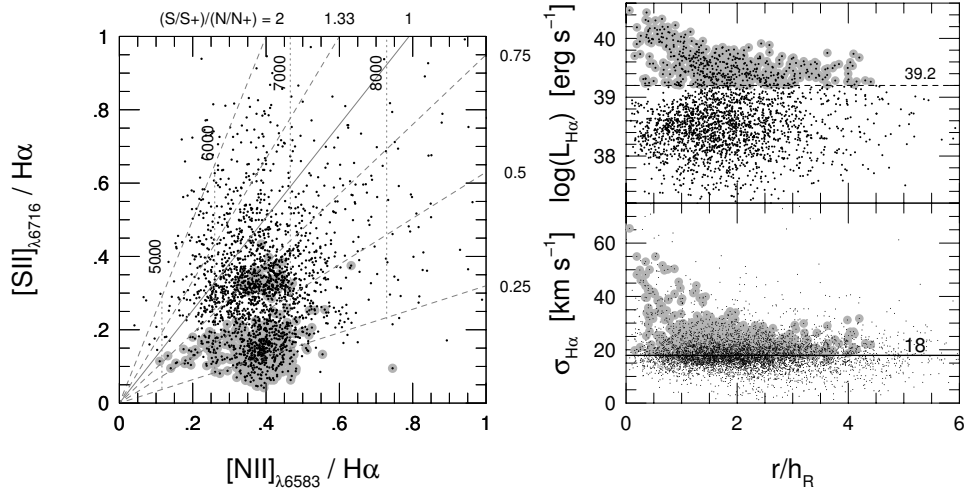


Figure 3. **Left Panel:** Line-ratios of [SII] and [NII] to $H\alpha$. Lines represent an extrapolation of the ionization-ratio model of Haffner et al. (1999), with vertical lines representing constant temperature (labeled), adopted from the model of Haffner et al. (1999). Note the bimodal distribution split roughly by $[SII]/H\alpha = 0.22$. **Right Panels:** $H\alpha$ luminosity (top) and velocity dispersions (bottom) vs radius for each fiber for all galaxies in our sample. Radii are normalized as in Figure 1. Note the bifurcation in luminosity at small radii. Fibers containing more than $\log(L_{H\alpha}) > 39.2$ are marked as larger, grey dots. These appear primarily at above-median σ and at low $[SII]/H\alpha$.

individual galaxies). Consequently, $[NII]/[SII]$ correlates positively with line-strength and line-width.

We also find the bivariate distributions of any two of $[SII]/H\alpha$, $[NII]/H\alpha$ and $L_{H\alpha}$ are bimodal about $L_{H\alpha} \sim 10^{39}$ ergs/s/kpc² or $[SII]/H\alpha \sim 0.2$ (Fig. 2 and 3). However, there is no bimodality in the distribution of any one of these parameters alone. While the physical interpretation of the range and bimodality in these line-ratios is unclear with extant data, Reynolds notes that a value of $[SII]/H\alpha \sim 0.22$ is roughly the demarcation between MW H II-regions and the DIG, and $[NII]/[SII] \sim 1.6$ gives a similar division (e.g., Haffner et al. 1999). Large values of $[SII]/H\alpha$ are typically indicative of shock heating in the diffuse gas, consistent with the lower $L_{H\alpha}$ in these regions. The bimodality, then, may be loosely interpreted as a physical division between H II-like regions and diffuse, DIG-like regions.

Variation in $[NII]/H\alpha$ is interpreted as arising from variations in metallicity or ionization parameter, with the latter favored by MW ISM studies of the DIG, and the former favored for H II regions in external galaxies. Without additional line diagnostics, given the coverage and sensitivity of our data, and hence the range of physical conditions likely sampled, it is unclear which

interpretation applies. Even if $[\text{NII}]/\text{H}\alpha$ is a reasonable metallicity index for luminosity-weighted measurements in systems dominated by H II regions, it should be applied with caution to the data considered here, particularly because $[\text{NII}]/[\text{SII}]$ has a much wider range than seen in the MW DIG (cf. Haffner et al. 1999). Whether this range represents variations in abundance, temperature, or ionization is subject of future inquiry. In this context, adding resolved measurements of H II galaxies into this analysis would be particularly useful, since Melnick et al. (1987) have long pointed out that these systems appear to be metal-poor versions of giant H II regions found in nearby, large galaxies.

Finally, we point out a bifurcation exists in $L_{\text{H}\alpha}$ vs radius (Fig. 3). Galaxies with steeply rising $L_{\text{H}\alpha}$ at small radii have strong σ gradients and $L_{\text{H}\alpha}$ above 10^{39} ergs/s/kpc². Consequently, these regions mostly have small $[\text{SII}]/\text{H}\alpha$ and large $[\text{NII}]/[\text{SII}]$. Further, it is these points that are found in the most rapidly rotating systems, such that V_{rot}/σ is lower even though σ is larger. Our line-ratio correlations with rotation are in general agreement with the long-slit measurements of Rubin, Ford, & Whitmore (1984). They argued their findings in terms of abundance variations due to a global-mass-dependent chemical enrichment history. Here, however, the trends are not based on means of individual galaxies or their luminosity-class, but on the conditions at a specific location within any given galaxy. The presence of radial gradients, and a quantitative threshold in $L_{\text{H}\alpha}$ on scales of ~ 1 kpc within individual galaxies, imply line ratios arise from local conditions within, rather than global properties of, galaxies. That this statement of locality and luminosity-dependence appears also to apply to ionized-gas line-widths may be a strong indication they have significant non-virial components.

Acknowledgments. This research was supported by NSF/AST-0307417 and enriched by discussion with M. Haffner, R. Reynolds, and the Diskmass group.

References

- Andersen, D. R. et al. 2001, ApJ, 551, L131
 Andersen, D. R., & Bershady, M. A. 2003, ApJ, 599, L79
 Andersen, D. R. et al. 2005, submitted to AJ
 Combes, F. & Bequaer, J.-F. 1997, A&A, 326, 554
 Haffner, M., Reynolds, R. J., Tufte, S. L. 1999, ApJ, 523, 223
 Jimenez-Vicente, J., et al. 1998, A&A, 342, 417
 Melnick, J. Terlevich, R., Moles, M. 1988, MNRAS, 235, 297
 Reynolds, R. J. 1988, ApJ, 333, 341
 Relano, M. et al. 2005, A&A, 431, 235
 Rozas, M. et al. 2000, A&A, 386, 42
 Rubin, V. C., Ford, W. K., Whitmore, B. C. 1984, ApJ, 281, L21
 Siegel et al. 2005, MNRAS, 356, 1117
 van der Kruit, P. C., & Shostak, G. S. 1982, A&A, 105, 351
 van der Kruit, P. C., & Shostak, G. S. 1984, A&A, 134, 258